

Particle method simulation of violent sloshing under rotational excitation

*M. Luo and C.G. Koh

Department of Civil and Environmental Engineering, National University of Singapore, Singapore 117576

†Corresponding author: ceelm@nus.edu.sg

Abstract

A three-dimensional (3D) numerical model is presented in the framework of Consistent Particle Method (CPM). The 3D gradient and Laplacian operators are derived based on Taylor series expansion, achieving good accuracy and largely alleviating the problem of spurious pressure fluctuation. Validated by our experimental study of water sloshing under rotational excitation, this model is shown to be robust and accurate in long time simulation of violent free surface flows which involve fluid merging and splitting.

Keywords: Particle method, Three-dimensional, Sloshing, Rotational Excitation.

Introduction

Liquid sloshing is a crucial issue in many engineering applications, one of which is the transportation of liquefied natural gas in membrane tanks on ships. The impact force induced by liquid sloshing may destroy the membrane layer and even cause structural failure of tank walls. In addition, large sloshing forces may capsize a ship when large overturning moments are generated. In this context, a better understanding of sloshing phenomenon is essential for the design of cost-effective LNG vessels.

With the rapid development of computer technology, numerical modelling has become increasingly feasible and many numerical algorithms have been developed to simulate sloshing problems. Among them are the mesh-based methods such as Finite Difference Method^{1,2}, Finite Volume Method³ and Finite Element Method⁴. These methods, however, may have some difficulties to model the large and discontinuous fluid motions which are generally involved in violent sloshing. In addition, the recognition or tracking of highly deformed free surface is also a tough issue (complicated and time-consuming) for mesh-based methods although some specialized schemes have been developed such as the Volume of Fluid⁵ and the level set method⁶.

In recent years, the particle methods such as Smoothed Particle Hydrodynamics (SPH), Incompressible Smoothed Particle Hydrodynamics (ISPH) and Moving Particle Semi-implicit (MPS) method have been developed and extensively used to model liquid sloshing as well as other free surface flows⁷⁻¹⁰. Because of the meshless nature, particle methods have better suitability in modelling merging and splitting of fluid and tracking of free surface. However, one of the challenging issues for these particle methods is the spurious pressure fluctuation. This is mainly caused by that the derivative approximation schemes in these methods which invoke a kernel function introduce numerical errors particularly for irregular particle distribution¹¹. To address this issue, a new particle method named Consistent Particle Method (CPM) has recently been proposed¹² by adopting the Generalized Finite Difference scheme¹³ to compute the spatial derivatives. Being consistent with Taylor series expansion and eliminating the use of a kernel function, CPM is fundamentally different from SPH, ISPH and MPS in terms of the derivative-approximation scheme. Due to the accurate computation of derivatives, the CPM solution of pressure history shows tremendous improvement over some

other particle methods¹², without the use of artificial viscosity or smoothing technique to remove spurious fluctuation.

In this context, the two-dimensional CPM is further developed into a 3D model. The accuracy of the developed numerical model is demonstrated by our experimental studies of violent water sloshing in a scaled tank under rotational excitation. The wave profiles, sloshing pressures at typical positions and the wave patterns are studied.

Consistent Particle Method

In particle methods, the fluid domain is represented by a collection of discrete Lagrangian particles, each of which carries a fixed mass and moves under external forces mainly arising from gravity and pressure difference. The governing equations are the Navier-Stokes equations in Lagrangian form as follows

$$\frac{1}{\rho} \frac{D\rho}{Dt} + \nabla \cdot \mathbf{v} = 0 \quad (1)$$

$$\frac{D\mathbf{v}}{Dt} = -\frac{1}{\rho} \nabla p + \nu \nabla^2 \mathbf{v} + \mathbf{g} \quad (2)$$

where ρ is the density of fluid, \mathbf{v} the particle velocity vector, p the fluid pressure, μ the dynamic viscosity of fluid and \mathbf{g} the gravitational acceleration.

In CPM, the above equations are solved by a predictor-corrector scheme. In the predictor step, the temporary particle velocities and positions are computed by neglecting the pressure gradient term. In the corrector step, a pressure Poisson equation (PPE) is solved as follows

$$\nabla \cdot \left(\frac{1}{\rho^*} \nabla p^{(k+1)} \right) = \frac{1}{\Delta t^2} \frac{\rho^{(k+1)} - \rho^*}{\rho^{(k+1)}} \quad (3)$$

The incompressibility condition is enforced by setting the fluid density at the current time step ($\rho^{(k+1)}$) to be the initial value (ρ_0). The intermediate fluid density (ρ^*) is evaluated based on the distance-weighted average of the masses of fluid particles including and around the reference particle¹⁴.

In CPM, the 3D gradient and Laplace operators in the governing equations are computed in the following way

$$\frac{\partial p_i}{\partial x} = \sum_{j \neq i} \left[w_j^2 \left(a_1 h_j + a_2 k_j + a_3 l_j + 0.5a_4 h_j^2 + 0.5a_5 k_j^2 + 0.5a_6 l_j^2 + a_7 h_j k_j + a_8 h_j l_j + a_9 k_j l_j \right) (p_j - p_i) \right] \quad (4)$$

$$\frac{\partial^2 p_i}{\partial x^2} = \sum_{j \neq i} \left[w_j^2 \left(d_1 h_j + d_2 k_j + d_3 l_j + 0.5d_4 h_j^2 + 0.5d_5 k_j^2 + 0.5d_6 l_j^2 + d_7 h_j k_j + d_8 h_j l_j + d_9 k_j l_j \right) (p_j - p_i) \right] \quad (5)$$

where i is the reference particle and j the neighbor particles in the influence domain, w_j is the weighting function used in the weighted-least-square scheme and is adopted to be the inverse distance function^{12, 13}. It is noted that this weighting function is essentially different from the

kernel function in SPH and ISPH (to approximate the Dirac delta function) and the weighting function in MPS (to specify the quantities diffused from the center particle to its neighbor particles). Similar to the two-dimensional CPM¹², $p_i = \min(p_j)$ for $\{j | r_{ij} \leq r_e\}$ is used in Equation (4) to improve the numerical stability. Similarly, the first derivatives in the y and z directions can be computed by replacing a_s ($s = 1, 2, \dots, 9$) in Equation (4) with b_s and c_s , whereas the second derivatives in the y and z directions can be computed by replacing d_s ($s = 1, 2, \dots, 9$) in Equation (5) with e_s and f_s . The coefficients $a_s, b_s, c_s, d_s, e_s, f_s$ ($s = 1, 2, \dots, 9$) can be obtained as

$$\begin{bmatrix} a_1 & a_2 & \dots & a_9 \\ b_1 & b_2 & \dots & b_9 \\ \vdots & \dots & & \vdots \\ f_1 & f_2 & \dots & f_9 \\ \vdots & \dots & & \vdots \end{bmatrix} = \left(\sum_{j \neq i} C_j \right)^{-1} \quad (6)$$

where

$$C_j = w_j^2 \begin{bmatrix} h_j^2 & h_j k_j & h_j l_j & 0.5h_j^3 & 0.5h_j k_j^2 & 0.5h_j l_j^2 & h_j^2 k_j & h_j^2 l_j & h_j k_j l_j \\ & k_j^2 & k_j l_j & 0.5h_j^2 k_j & 0.5k_j^3 & 0.5k_j l_j^2 & h_j k_j^2 & h_j k_j l_j & k_j^2 l_j \\ & & l_j^2 & 0.5h_j^2 l_j & 0.5k_j^2 l_j & 0.5l_j^3 & h_j k_j l_j & h_j l_j^2 & k_j l_j^2 \\ & & & 0.25h_j^4 & 0.25h_j^2 k_j^2 & 0.25h_j^2 l_j^2 & 0.5h_j^3 k_j & 0.5h_j^3 l_j & 0.5h_j^2 k_j l_j \\ & & & & 0.25k_j^4 & 0.25k_j^2 l_j^2 & 0.5h_j k_j^3 & 0.5h_j k_j^2 l_j & 0.5k_j^3 l_j \\ & & & & & 0.25l_j^4 & 0.5h_j k_j l_j^2 & 0.5h_j l_j^3 & 0.5k_j l_j^3 \\ & & sym & & & & h_j^2 k_j^2 & h_j^2 k_j l_j & h_j k_j^2 l_j \\ & & & & & & & h_j^2 l_j^2 & h_j k_j l_j^2 \\ & & & & & & & & k_j^2 l_j^2 \end{bmatrix}$$

The free surface particles are recognized by the 3D spoke method developed by Luo et al¹⁵. The fixed particle approach is adopted to model the wall boundaries.

Water sloshing under rotational excitation

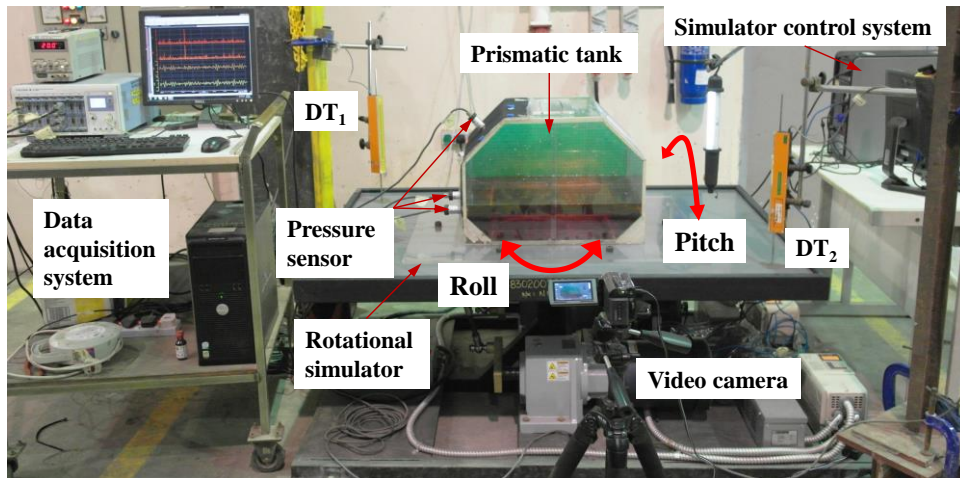


Figure 1. Water sloshing on rotational simulator

obtain the actual roll and pitch motions of the simulator, the vertical displacements at two diagonally opposite points on the simulator platform are measured by two vertically positioned displacement transducers (DT₁ and DT₂ in Figure 1 and Figure 2). Both displacement and pressure signals are recorded by a digital oscilloscope.

The excitation frequencies of roll and pitch rotations are set to be the same as the corresponding natural frequencies, i.e. 5.598 rad/s and 7.471 rad/s respectively. The measured rotations for the two directions are as shown in Figure 4. The pitch motion is not sinusoidal because of the control precision of the simulator. However, this does not influence the results since the real motions are used as the input of numerical simulations. In the numerical model, an initial particle spacing of 0.008 m (116,361 particles in total) and fixed time step of 0.0005 s are used. The wave profiles at different time instants are presented in Figure 5, showing generally good agreement between the numerical and experimental results. In the beginning, a swirling wave that rotates anticlockwise (viewed from top) is generated in the tank. Wave breaking occurs on the left wall of the tank at about 1.96 s. After $t = 2.40$ s, the swirling wave changes its direction to be clockwise which can be seen from the snapshots progressively from 2.40 s to 2.86 s. From about 5.26 s to 5.80 s, the swirling wave becomes anticlockwise again. The swirling wave can be explained by the superposition of the wave components in the length and breadth directions as

$$A(x, y) = A_x \cdot f_{1,0}(x, y) \cdot \sin(\omega_x t + \varphi_x) + A_y \cdot f_{0,1}(x, y) \cdot \sin(\omega_y t + \varphi_y) \quad (7)$$

where $f_{1,0}(x, y)$, A_x , ω_x and φ_x are respectively the first modal shape of the wave, amplitude of wave elevation, and the frequency and phase angle of the wave in the length direction, whereas $f_{0,1}(x, y)$, A_y , ω_y and φ_y are those parameters in the breadth direction. Because ω_x and ω_y are different, the swirling wave changes its rotary direction cyclically (with a “beating” frequency of $|\omega_x - \omega_y|$), which can also be seen from the pressure result presented in Figure 6. This observation is different from the sloshing phenomenon under 1-degree-of-freedom translational excitation¹⁶, in which the rotary direction of swirling is dependent on the initial perturbation of wave and theoretically does not change.

A practical significance is that swirling waves generate large impact force near the corner of the tank as presented in Figure 6, which shows the sloshing pressures at P₁ and P₂. Due to the impact of swirling wave at the tank corner, the impact pressure at P₂ is larger than that at P₁ at the middle of the wall. 3D-CPM captures this phenomenon with the numerical results in generally good agreement with the experimental results. In particular, the large impact peaks at the tank corner are accurately predicted by the CPM as can be seen from the enlarged view of Figure 6. The relative difference between the CPM and experimental results is only 3.9% for the largest pressure peak. Some minor discrepancies exist between the numerical and experimental results of sloshing pressure at the reversals of swirling direction, the reason for which is as follows. The changes of wave swirling direction correspond to the changes of rotational direction of the simulator, which implies larger rotational accelerations. Since the tip of the displacement transducer is in contact with the top surface of the platform, friction force exists between the transducer and the platform when rotational acceleration of the platform is larger, thereby inducing errors in the measured rotational angles (particularly when there is a reversal of rotation). Since the measured rotational angles of the rotational simulator are used as the input of CPM simulation, such errors are brought into the numerical simulation. Although measures were taken to minimise the friction force between the

displacement transducer and the platform, it was not possible to completely eliminate this experimental error.

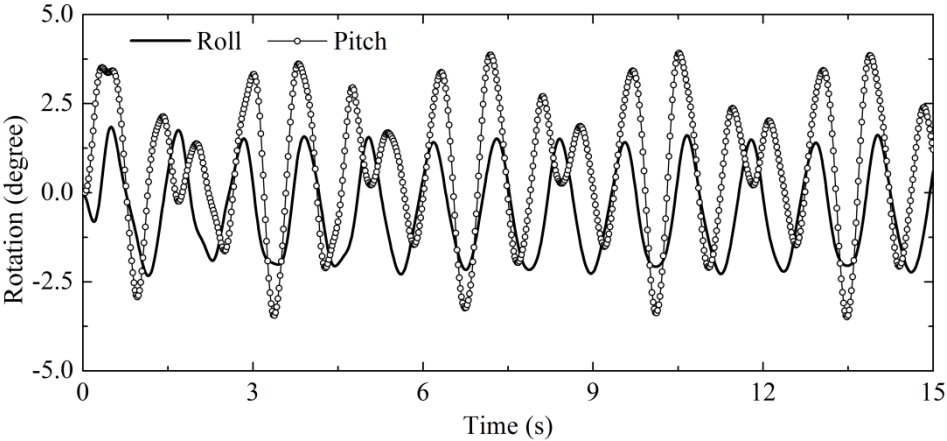


Figure 4. Water sloshing under resonant rotational excitation: roll and pitch angles

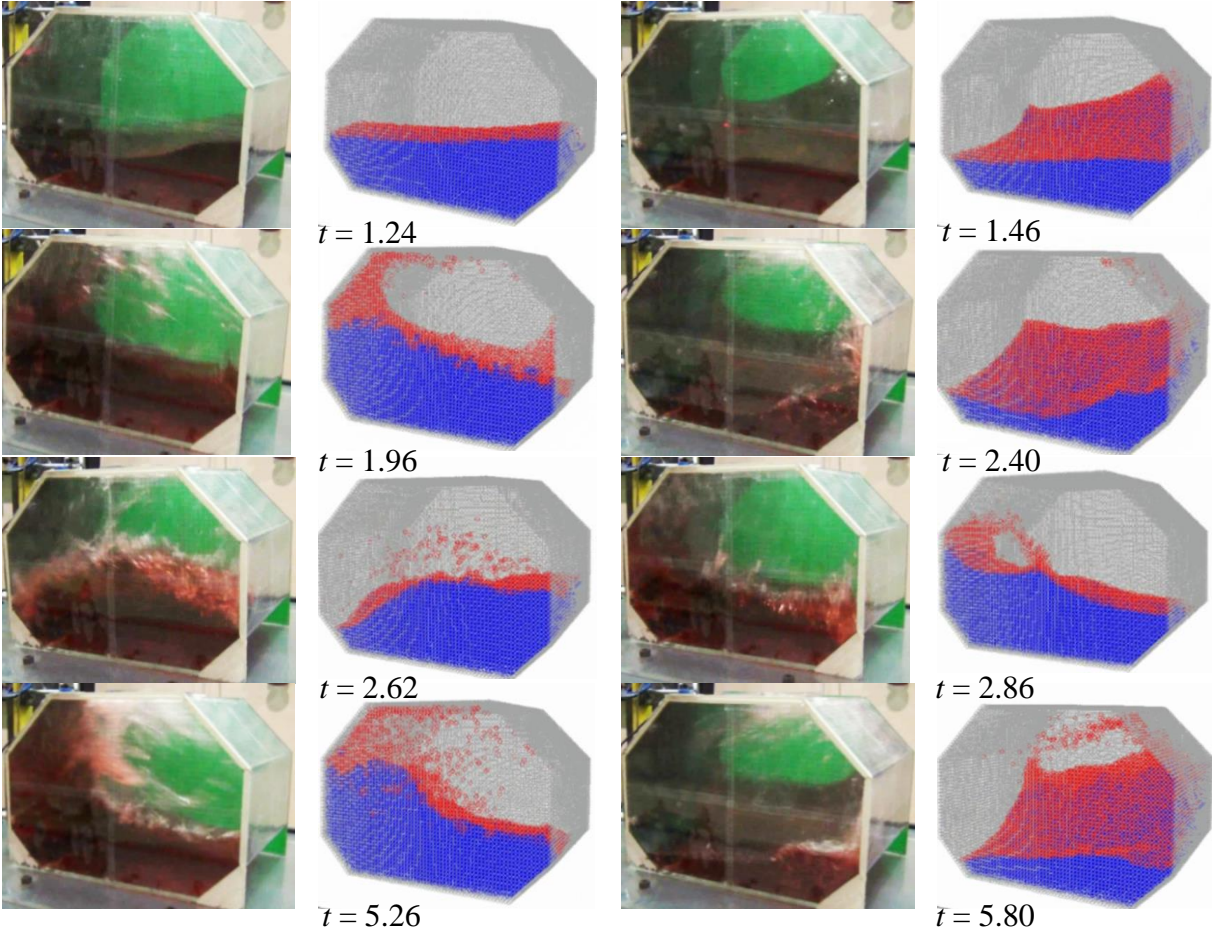


Figure 5. Water sloshing under resonant rotational excitation: wave profiles at typical time instants

Conclusions

In this study, the recently developed CPM is extended to simulate 3D sloshing waves. The 3D spatial derivatives are computed in a way consistent with Taylor series expansion, producing good accuracy even for irregular particle distributions. The 3D CPM is used to simulate the

water sloshing in a scaled tank under rotational excitations. These complex wave motions and the sloshing pressures predicted by the 3D CPM are in fairly good agreement with the experimental results.

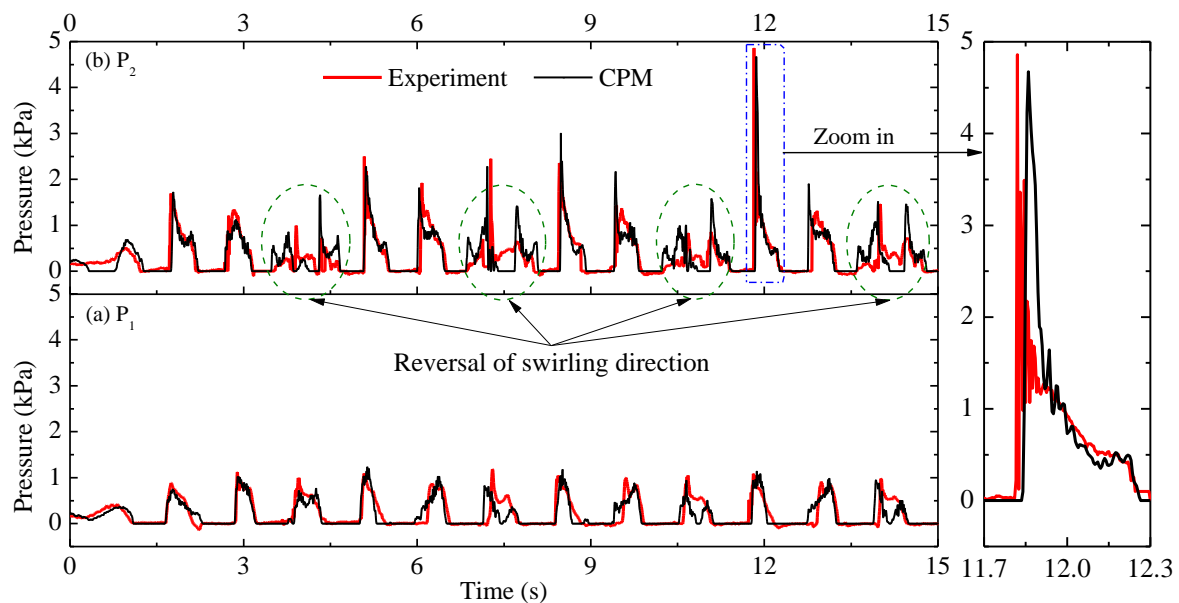


Figure 6. Water sloshing under resonant rotational excitation: pressure histories at P_1 and P_2

Acknowledgement

The authors appreciate the research grant provided by the Singapore Maritime Institute (Project SMI-2014-OF-02) as well as the funding and technical support of Sembcorp Marine Technology Pte Ltd.

References

- [1] Liu D, Lin P. A numerical study of three-dimensional liquid sloshing in tanks. *Journal of Computational Physics* 2008;227:3921-39.
- [2] Xue MA, Lin P. Numerical study of ring baffle effects on reducing violent liquid sloshing. *Computers & Fluids* 2011;52:116-29.
- [3] Marsooli R, Wu W. 3-D finite-volume model of dam-break flow over uneven beds based on VOF method. *Advances in Water Resources* 2014;70:104-17.
- [4] Wang CZ, Khoo BC. Finite element analysis of two-dimensional nonlinear sloshing problems in random excitations. *Ocean Engineering* 2005;32:107-33.
- [5] Hirt CW, Nichols BD. Volume of fluid (VOF) method for the dynamics of free boundaries. *Journal of Computational Physics* 1981;39:201-25.
- [6] Sussman M, Smereka P, Osher S. A level set approach for computing solutions to incompressible two-phase flow. *Journal of Computational Physics* 1994;114:146-59.
- [7] Shao S, Lo EYM. Incompressible SPH method for simulating Newtonian and non-Newtonian flows with a free surface. *Advances in Water Resources* 2003;26:787-800.
- [8] Koshizuka S, Nobe A, Oka Y. Numerical analysis of breaking waves using the moving particle semi-implicit method. *International Journal for Numerical Methods in Fluids* 1998;26:751-69.
- [9] Shao JR, Li HQ, Liu GR, Liu MB. An improved SPH method for modeling liquid sloshing dynamics. *Computers & Structures* 2012;100-101:18-26.
- [10] Liu X, Lin P, Shao S. An ISPH simulation of coupled structure interaction with free surface flows. *Journal of Fluids and Structures* 2014;48:46-61.
- [11] Luo M, Koh CG, Gao M, Bai W. A particle method for two-phase flows with large density difference. *International Journal for Numerical Methods in Engineering* 2015;103:235-55.

- [12] Koh CG, Gao M, Luo C. A new particle method for simulation of incompressible free surface flow problems. *International Journal for Numerical Methods in Engineering* 2012;89:1582–604.
- [13] Liszka T, Orkisz J. The finite difference method at arbitrary irregular grids and its application in applied mechanics. *Computers & Structures* 1980;11:83-95.
- [14] Koh CG, Luo M, Gao M, Bai W. Modelling of liquid sloshing with constrained floating baffle. *Computers & Structures* 2013;122:270-9.
- [15] Luo M, Koh CG, Bai W. A three-dimensional particle method for violent sloshing under regular and irregular excitations. *Ocean Engineering* 2016;120:52-63.
- [16] Faltinsen OM, Rognebakke OF, Timokha AN. Classification of three-dimensional nonlinear sloshing in a square-base tank with finite depth. *Journal of Fluids and Structures* 2005;20:81-103.